FGFR1, Signaling, and AP-1 Expression after Retinal Detachment: Reactive Müller and RPE Cells

Scott F. Geller,[1,2] *Geoffrey P. Lewis,*[2] *and Steven K. Fisher*[1,2]

Purpose. To identify changes in cellular signaling pathways and AP-1 expression in retina and retinal pigmented epithelium (RPE) after experimental retinal detachment (RD).

Methods. Cat and rabbit neural retinas were separated from the RPE in vivo for 5 minutes to 28 days. Tissues were removed and processed for Western blotting, immunohistochemistry, in situ hybridization, and immunoprecipitation experiments.

Results. An ordered sequence of events occurs after RD: (1) fibroblast growth factor (FGF) receptor 1 (FGFR1, flg) is phosphorylated in the retina within 15 minutes and dephosphorylated 2 hours after RD; (2) The extracellular signal-regulated kinase (ERK) is phosphorylated in both Müller and RPE cells within 15 minutes and remains so for several days; (3) De novo expression of *c-fos* mRNA coincides with increased c-Fos and c-Jun immunoreactivity in both Müller and RPE cells; (4) CREB is phosphorylated in a subpopulation of photoreceptors; and (5) STAT3 and NF-κB are activated in inner nuclear layer cells by 1 day of RD.

Conclusions. These data suggest that nonneuronal cells (RPE and Müller cells) respond to RD very rapidly by stimulating ERK signaling and AP-1 transcription factor expression. Furthermore, these data suggest that basic fibroblast growth factor (FGF-2, bFGF) is involved in initiating the retina's earliest responses to RD. The events described here precede changes in gene expression and morphology that can have serious effects on visual outcome in humans treated for retinal detachment or other retinal injuries. (*Invest Ophthalmol Vis Sci.* 2001;42: 1363–1369)

Retinal detachment (RD), the physical separation of the neural retina from the retinal pigmented epithelium (RPE), is a common ocular injury that often leads to visual impairment and in some cases blindness. If the macula (central retina) is detached for a few days, successful surgical reattachment produces a final visual acuity of 20/50 or better in approximately 39% of patients.[1,2] Using an animal model of RD, we have demonstrated a series of predictable cellular events occurring within 3 days of detachment, all of which have the potential to negatively affect final visual outcome: loss of structural integrity and apoptotic death of photoreceptor cells, neurite outgrowth from second-order neurons, proliferation of nonneuronal cell types, and extensive hypertrophy of Müller cells.[3–8] In addition to growing and dividing, Müller cells routinely increase intermediate filament expression and grow specifically into the subretinal space, suggesting that many responses to RD are highly coordinated and regulated.[6,9]

Although many factors have been shown to be protective for photoreceptors after retinal injury,[10–12] the release of endogenous growth factors after RD may also contribute to the well-defined gliotic response of Müller cells. Basic fibroblast growth factor (FGF-2) is one of several agents that elicit profound effects in retinal cells. We have shown previously that FGF-2 injection into normal eyes induces Müller cell reactivity similar to that observed in response to RD,[9] and FGF-2 has recently been shown to activate ERK, a mitogen-activated protein kinase (MAPK), in Müller cells.[13] Cellular stress, growth factors, and MAPK signaling cascades are each capable of inducing de novo expression of immediate-early response genes such as c-Fos and c-Jun. Both c-Fos and c-Jun are components of the activator protein (AP)-1 transcription factor, a pivotal regulator of gene expression in a variety of both normal and abnormal cellular processes.[14–17]

In the present study we have identified multiple reactive signaling responses after experimental RD, including phosphorylation of FGFR1, a high-affinity receptor for FGF-2, ERK signaling, and extended AP-1 expression. It is important to identify factors and signaling events after RD to develop and assess methods to minimize cellular damage/death and gliosis, and to enhance retinal regeneration after injury. Moreover, studying the immediate effects of RD has recently assumed new significance because clinically induced RD followed by macular translocation has become a key part of an experimental therapy for treatment of age-related macular degeneration.[18,19]

Materials and Methods

Experiments were performed with cats (*Felis domesticus*) and rabbits (New Zealand White). All procedures used were in accordance with the guidelines provided by the ARVO Statement for the Use of Animals in Ophthalmic and Vision Research and with the approval of the UCSB Animal Care Council.

Retinal Detachments

Sixteen adult cats and 16 adult rabbits (duplicate animals for each time point) were anesthetized with 18 mg/kg or 15 mg/kg Ketaset (ketamine HCl; Parke-Davis, Morris Plains, NJ) and 1.2 or 3 mg/kg Rompun (xylazine; Miles Laboratories, Shawne, KS), respectively. Upon deep anesthesia, experimental retinal detachments were performed as described previously.[20] A detachment approximately one half the size of the entire retina was made in each experimental eye. Cats were euthanatized at 15 minutes, 2 hours, 1 day, 3 days, 7 days, and 28 days, whereas rabbits were euthanatized at 5 minutes, 15 minutes, 30 minutes, 2 hours, 4.5 hours, 1 day, and 3 days after the detachment surgery. The presence and extent of each detachment was confirmed by direct observation once the anterior eye structures were removed. Sham operations were not performed; however, left eyes served as normal (nondetached) control tissue.

Tissue Processing

After IV overdose with sodium pentobarbital, whole eyes were removed and either placed into fixative (4% paraformaldehyde in PBS,

From the [2]Neuroscience Research Institute and the [1]Department of Molecular, Cellular, and Developmental Biology, University of California, Santa Barbara.

Supported by National Institutes of Health Grant EY00888 (SKF).

Submitted for publication September 26, 2000; revised January 3, 2001; accepted January 24, 2001.

Commercial relationships policy: N.

The publication costs of this article were defrayed in part by page charge payment. This article must therefore be marked *"advertisement"* in accordance with 18 U.S.C. §1734 solely to indicate this fact.

Corresponding author: Scott F. Geller, Anatomy and Histology, University of Sydney F13, Sydney, NSW, Australia 2006.
sgeller@anatomy.usyd.edu.au

pH 7.4) or bisected; one half was placed into fixative to be used for immunohistochemistry and in situ hybridization, and the complementary half globe was dissected for biochemical analysis. For all immunohistochemical procedures, small pieces (~5 × 5 mm) of normal and detached retinal and RPE tissues were fixed for at least 24 hours at 4°C, excised, and embedded in wax as described previously.[6] For biochemical analysis, the detached portion of retina from the unfixed half globe was dissected and homogenized in 200 to 300 μl of a protease and phosphatase-inhibiting buffer. Protein concentrations were determined for each supernatant using the BCA assay (Pierce, Rockford, IL).

Antibodies

Several antibodies were used in the experiments: anti-p42/p44 MAP kinase (ERK; SC-93; Santa Cruz Biologicals [SCB], Santa Cruz, CA); anti–phospho-ERK (pERK; 9101S; New England Biolabs [NEB], Beverly, MA); anti- c-Fos (SC-52; SCB); anti–pan-Fos (c-Fos and Fos-related antigens [FRA];SC-253; SCB); anti- c-Jun (SC-1649; SCB); anti–phospho-c-Jun (pJun; 9261S; NEB); anti-vimentin (M725; Dako Corporation, Carpinteria, CA); anti-FGFR1 (Flg; SC-121; SCB); anti–phospho-signal transducer and activator of transcription (pSTAT3; 9131S; NEB); anti–phospho-Ca^{2+}/cAMP response element binding protein (pCREB; 9191S; NEB); anti-nuclear factor-kappa B (NF-κB [activation specific]; 1697838; Boehringer Mannheim, Indianapolis, IN), and agarose-conjugated anti-phosphotyrosine (PY99-AC; SC-7020; SCB). All antibodies were titered to show specific labeling with low background staining. Antibody dilutions were between 1/50 and 1/200 for immunohistochemistry and were 1/1000 for Western blotting, with the diluent being phosphate-buffered saline (PBS) with 0.1% to 0.2% Tween-20 and 0.5% BSA, pH 7.4.

Immunohistochemistry

Four-micrometer-thick sections of retinal tissues were placed on ProbeOn Plus capillary gap microscope slides (Fisher Scientific, Pittsburgh, PA). For consistency, all immunohistochemical procedures were performed using an automated histostainer (Ventana Medical Systems, Tucson, AZ) as described previously with minor modifications.[6] Tissue sections were enhanced for antigenicity,[21] and protein localization was visualized using DAB. For double-labeling experiments, the FRA antibody was used in conjunction with a monoclonal antibody to vimentin, which was detected using an alkaline phosphatase–based red reaction product, easily distinguishable from the dark brown DAB precipitate (identifying FRA immunolabeling). After rinsing with water, the slides were dehydrated into xylenes, and a coverslip was applied with Permount (Fisher Scientific). Sections were photographed using Nomarski optics.

Immunoprecipitation

Fifty micrograms (50 μl) of each Triton X-100 extracted cat retinal homogenate was added to 50 μl of 100 mM Tris/1% SDS (pH 7.2), boiled for 2 minutes, chilled on ice, and mixed with 100 μl of 100 mM Tris/5% Triton X-100 (pH 7.2). Ten microliters (20 μg) of agarose beads conjugated to anti-phosphotyrosine antibodies was added, and the tubes were tumbled for 24 hours at 4°C. Beads were washed with homogenization buffer (three times for 5 minutes), mixed with 50 μl of 100 mM Tris/2% SDS/25% glycerol (pH 7.5; for 5 minutes), vortexed briefly, and spun at 16,600*g* for 5 minutes. The supernatant was removed and added to fresh tubes containing 1 μl BME and 2 μl DTT (100 mM). The samples were then boiled for 90 seconds and loaded onto a 9% polyacrylamide SDS gel. Electrophoresis and immunoblotting were performed as described below (Western blot analysis) using a primary antibody to FGFR1.

Western Blot Analysis

Western blotting was done according to standard SDS-PAGE protocol. Briefly, 25 μg of each homogenate was loaded onto a 10% polyacrylamide gel. After transfer to nitrocellulose, the separated proteins were treated with 0.5% ponceau S (Sigma, St. Louis, MO) to observe the loading and electrophoretic separation of each homogenate, and all lanes appeared to be evenly loaded. The blots were incubated with antibodies to pERK or c-Jun at 1:1000 overnight in a sealed bag, followed by an HRP-conjugated secondary antibody and detected with Supersignal West Pico chemilluminescent reagents (Pierce) using Hyperfilm ECL film (Amersham Pharmacia Biotech, Inc., Piscataway, NJ).

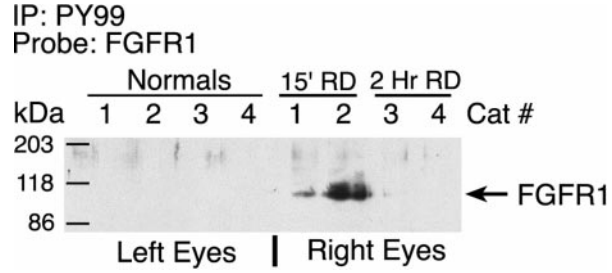

Figure 1. FGFR1 becomes phosphorylated in response to RD. Homogenates were immunoprecipitated with anti-phosphotyrosine, electrophoresed, and probed with an antibody to FGFR1. *Right four lanes*: FGFR1 is phosphorylated at 15 minutes after RD (right eyes, cats 1 and 2), and dephosphorylated by 2 hours after RD (right eyes, cats 3 and 4). *Left four lanes*: paired control (left eyes) eyes showed no immunoreactivity. Apparent kDa of the bands are 110 (cats 1 and 2) and 118 kDa (cat 2).

In Situ Hybridization

Digoxygenin-labeled riboprobes were synthesized from a human *c-fos* EST cloned into Bluescript pBSK$^-$ (a gift from Steve Benson, UCSF; ATCC 135445). Sense and antisense riboprobes were synthesized using the T3 and T7 RNA polymerases. All riboprobes were subsequently precipitated, resuspended, quantified, and resuspended in hybridization solution[22] at 1 μg/ml. Eight-micrometer-thick wax sections of retinal and RPE tissues were cleared with xylenes and rehydrated stepwise into PBS. Sections were treated according to published procedures for prehybridization treatment,[22] dehydrated, and air-dried. Prehybridization solution was applied and allowed to incubate for 2 hours at 59°C, followed by addition of sense or antisense digoxygenin-labeled riboprobes at 59°C overnight. Tissue sections were stringently washed with 0.1× SSC at 60°C for 2 hours, blocked with 3% BSA, and incubated with an anti-digoxygenin antibody (Boehringer Mannheim) conjugated to alkaline phosphatase at 1:1000 for 2 hours. NBT (nitro BT; Fisher Scientific) and BCIP (5-bromo-4-chloro-3-indolyl phosphate; Fisher Scientific) in Tris buffer (pH 9.4) was added, and the sections were incubated for up to 24 hours in the dark.

Results

FGFR1 Phosphorylation

Immunoprecipitating tyrosine-phosphorylated proteins from cat retinal homogenates, followed by Western blotting for FGFR1 shows no detectable FGFR1 phosphorylation in the four normal retinas (Fig. 1). Distinctive bands at approximately 110 kDa (cat 1) and 110/118 kDa (cat 2) are observed in retinas detached for 15 minutes, whereas no immunoreactivity was observed in either of the retinas detached for 2 hours (cats 3 and 4). In a longer exposure of the same blot, a band at approximately 110 kDa was visualized in one 2-hour RD (cat 3, data not shown), indicating that a low level of FGFR1 phosphorylation occurs for at least a couple of hours after RD.

p42/p44 MAP Kinase (ERK) Immunohistochemistry

Sections treated with secondary antibodies alone show no immunoreactivity (Fig. 2A). ERK immunohistochemistry in nor-

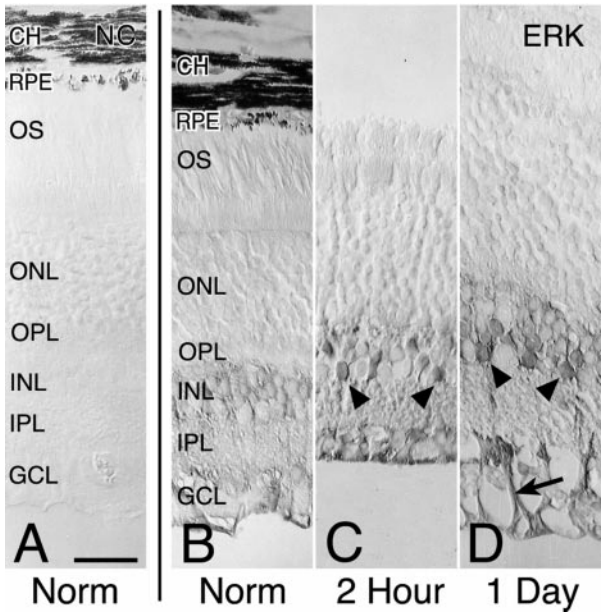

FIGURE 2. Immunohistochemical analysis of cat retina probed with an antibody to ERK indicates a translocation of ERK to the nuclear compartment. (**A**) No labeling with secondary antibody alone (negative control; NC) in normal cat retina. Normal retina (**B**) shows light ERK labeling throughout, with slightly more immunoreactivity in the inner retina (GCL, IPL, INL). Both 2 hours (**C**) and 1 day (**D**) detachments cause ERK to be localized in nuclei (*arrowheads*; **C**, **D**) and cytoplasm of Müller cells (*arrow*; **D**). CH, choriocapillaries; OS, photoreceptor outer segments. Scale bar, (**A** through **D**) 30 μm.

mal retina (Fig. 2B) shows a low level of labeling primarily restricted to the inner retina: the ganglion cell layer (GCL), inner plexiform layer (IPL), and inner nuclear layer (INL). In retinas detached for 2 hours, labeling increases in INL cell bodies and nuclei (arrowheads, Fig. 2C), as well as in Müller cell endfeet in the GCL. INL (arrowheads, Fig. 2D) and Müller cell endfoot (arrow, Fig. 2D) labeling continues at 1 day and returns to near normal levels by 7 days (data not shown).

Phosphorylated-ERK Immunohistochemistry

Very light pERK labeling is apparent throughout the normal retina, with slightly elevated immunoreactivity in some Müller cell endfeet (arrowhead, Fig. 3A). pERK labeling increases within 15 minutes in INL cell bodies (arrowheads, Fig. 3B) and Müller cell endfeet (arrows, Fig. 3B). A further increase in staining intensity occurs in the same pattern at 2 hours (Fig. 3C). pERK labeling decreases and returns to near normal levels by 28 days after RD (Figs. 3D through 3G). Anti-pERK does not label normal cat RPE cells (Fig. 3H); however, 15 minutes after RD (arrowheads, Fig. 3I), many RPE cells become immunopositive. Normal rabbit retina shows a very light, diffuse labeling (Fig. 3J), and Müller cell–specific labeling (arrows, Fig. 3K) appears 15 minutes after RD, similar to the cat. Immunoblotting with anti-pERK (Figs. 3L, 3M, upper panels) reinforces the finding that ERK activation occurs within minutes of RD in both the cat (Fig. 3L) and the rabbit (Fig. 3M). Reprobing the blots with an antibody to ERK indicates even loading of the gels (lower panels).

c-fos In Situ Hybridization and c-Fos Immunohistochemistry

Normal (Figs. 4A, 4C) and 2 hours' detached (Figs. 4B, 4D) retinal sections were hybridized with sense or antisense digoxygenin-labeled *c-fos* riboprobes. Labeling is absent except for a distinct antisense hybridization signal in the INL, 2 hours after RD (arrows, Fig. 4D). Antisense hybridization in sections of cat RPE (Figs. 4E through 4J) shows increased *c-fos* mRNA expression at 15 minutes (arrowheads, Fig. 4H) and above normal expression 2 hours after RD (arrowheads, Fig. 4J).

Normal retina shows very low levels of c-Fos immunolabeling (Fig. 5A). Increased c-Fos immunoreactivity is apparent in INL cells at 2 hours (Fig. 5C). The intensity and number of labeled cells peaks in retinas detached for 1 day (arrows, Fig. 5D), with a progressive decline at later time points (Figs. 5E through 5G). Increased c-Fos immunoreactivity is apparent in some GCL cells (arrows, Fig. 5F) but only the rare photoreceptor shows any labeling with the c-Fos specific antibody (arrowhead, Fig. 5D).

Immunolabeling with the pan-Fos antibody (FRA) demonstrates a similar time course and cell specificity, but the labeling is routinely more intense than with the c-Fos–specific antibody, indicating that other Fos family members may also be expressed in the retina (data not shown). FRA expression is increased both in the cat RPE (Figs. 5H, 5I) and rabbit retina

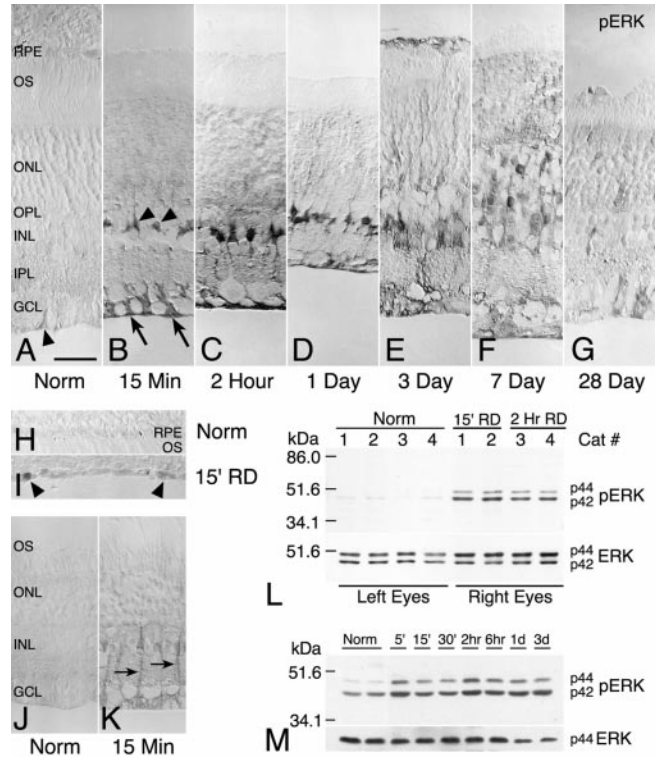

FIGURE 3. ERK becomes phosphorylated in retina and RPE in both cat and rabbit after RD. In normal cat retina (**A**), very light pERK immunolabeling is restricted to Müller cell bodies and endfeet (*arrowhead*). After RD (**B** through **G**), pERK immunoreactivity is observed in Müller cell endfeet (*arrows*; **B**) and cell bodies (*arrowheads,* **B**) within 15 minutes and becomes more intense at 2 hours (**C**). An increase in pERK immunoreactivity is also seen at 1 (**D**), 3 (**E**), and 7 days (**F**) after RD but declines to near normal levels by 28 days (**G**). pERK immunoreactivity is also present in cat RPE within 15 minutes of RD (*arrowheads*; **I**) but not in normal RPE (**H**). Detached rabbit retina demonstrates a similar response with pERK immunolabeling appearing in Müller cells within 15 minutes (*arrows*; **K**). (**L** and **M**) Western blot analysis of pERK induction after RD in cat and rabbit, respectively. In the cat (**L**), ERK is phosphorylated at both 15 minutes and 2 hours in experimental (right) eyes but not in the paired control (left) eyes (*top panel*). In the rabbit (**M**), ERK is phosphorylated above normal levels (*left 2 lanes, top panel*) at all time points between 5 minutes and 3 days of RD. Scale bar, (**A** through **G**, **J**, and **K**) 30 μm; (**H** and **I**) 25 μm.

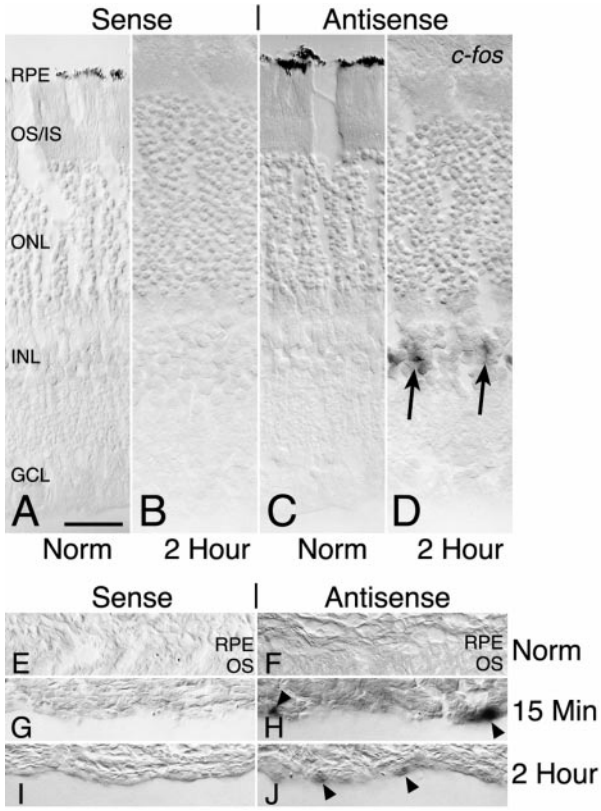

FIGURE 4. c-fos mRNA expression increases in RPE and INL cells within 15 minutes and 2 hours of retinal detachment, respectively. The digoxygenin-labeled sense riboprobe (**A**, **C**, **E**, **G**, **I**) shows no hybridization, whereas the antisense riboprobe (**B**, **D**, **F**, **H**, **J**) hybridizes specifically to cells in the INL at 2 hours (*arrows*; **D**) and to RPE cells at 15 minutes (**H**) and 2 hours (**J**) after RD (*arrowheads*; **H**, **J**). Scale bar, (**A** through **J**) 30 μm.

(Figs. 5J, 5K; arrowheads indicate photoreceptor labeling) 2 hours after RD.

Double labeling of normal and detached (Figs. 5L, 5M) rabbit retinas with anti-FRA and anti-vimentin, an intermediate filament protein whose expression increases in Müller cells in response to RD,[23] confirms that Müller cells become FRA positive. Vimentin labeling (arrows, Fig. 5M) increases and surrounds FRA-positive Müller cells (arrowheads, Fig. 5M) 4.5 hours after RD. By direct observation, the antibodies were distinguished using differently colored chromagen substrates.

c-Jun Immunohistochemistry

c-Jun Immunolabeling (Fig. 6) shows a nearly identical time course and pattern of induced immunoreactivity as that seen for c-Fos (Fig. 5). INL cells show increased c-Jun immunoreactivity 2 hours after RD (arrowheads, Figs. 6C, 6D). Prominent c-Jun labeling continues in the INL through 7 days, and some ganglion cells also show higher than normal immunoreactivity after RD (arrow, Fig. 6E). Labeling in detached rabbit retina (Figs. 6H, 6I) is comparable to that in the cat, including the frequent INL cells (arrowheads, Fig. 6I) and the occasional ganglion cell (arrow, Fig. 6I). Cat RPE responds similarly, showing no labeling in normal RPE (Fig. 6J) and distinct labeling 2 hours after RD (arrowheads, Fig. 6K).

Immunoblotting cat retinal homogenates indicates c-Jun induction in two eyes with 2-hour RD's (Fig. 6L). Immunolabeling with an antibody specific to the phosphorylated (activated) form of c-Jun (pJun) appears within 2 hours of RD in the INL (arrow, Fig. 6N). Although the intensity of pJun labeling is light, the pattern of immunolabeling is virtually identical with that for c-Jun immunohistochemistry (Fig. 6D).

pSTAT3, pCREB, and Active NF-κB Immunohistochemistry

Labeling with the phospho-STAT3 (pSTAT3) antibody shows no immunoreactivity in normal cat RPE (Fig. 7A), whereas 3 days after RD (arrowheads, Fig. 7B), some RPE cells are pSTAT3 immunopositive. Although normal cat retina shows no immunoreactivity for pSTAT3 (Fig. 7C), very light pSTAT3 labeling is seen in some INL cells by 1 day (Fig. 7D), with more intense labeling at 3 days (Fig. 7E). pSTAT3 immunolabeling declines at 7 days after RD (Fig. 7F), and by 28 days (Fig. 7G) the labeling is comparable to that seen in normal retina. The phospho-CREB (pCREB) antibody labels cells in the INL and GCL of normal and detached retina (Figs. 7H through 7L). At both 1 and 3 days after RD there are occasional scattered pCREB immunopositive photoreceptors (arrowheads), and increased labeling is apparent in some INL cells (Figs. 7I, 7J). An antibody to activated NF-κB shows a low level of labeling in all layers of normal retina (Fig. 7M). At 1 and 3 days (Figs. 7N, 7O), there is increased immunolabeling of activated NF-κB in a subset of cells in the INL and GCL. Labeling intensity decreases at 7 days (Fig. 7P) and approaches control levels by 28 days (Fig. 7Q).

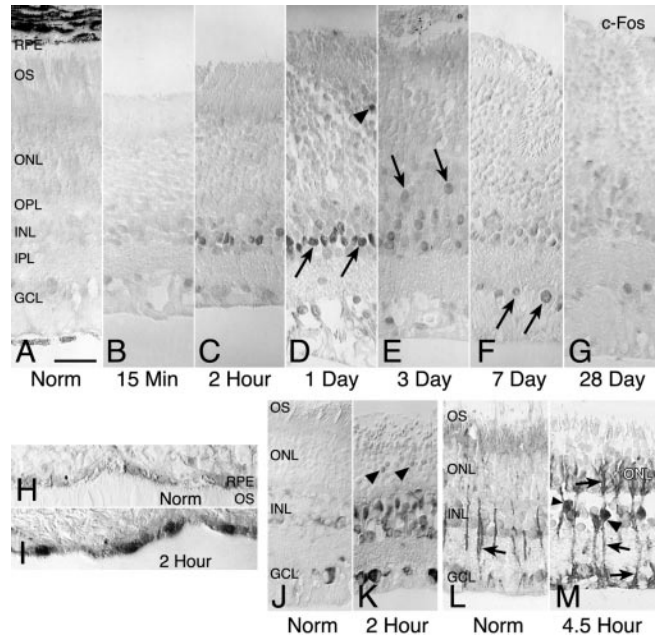

FIGURE 5. c-Fos immunolabeling increases in response to RD. Normal (**A**) and 15 minutes detached cat retina (**B**) show very light labeling throughout the retina. Dramatically increased c-Fos labeling is detected at 2 hours (**C**), 1 day (**D**), and 3 days (**E**) after RD in the INL. Even at 7 (**F**) and 28 days (**G**) after detachment, some increased c-Fos labeling is observed. c-Fos immunoreactivity peaks around 1 day (**D**), where a continuous string of cells (*arrows*) is labeled in the INL, and a positively labeled photoreceptor cell is identified in the ONL (*arrowhead*). *Arrows* in (**E**) identify cells likely to be migrating Müller cells; *arrows* in (**F**) identify c-Fos–positive cells in the GCL. An antibody that detects all members of the Fos family (c-Fos and Fos-related antigens, FRAs) was used in (**H**) through (**M**). FRAs are induced in RPE cells within 2 hours after RD (**I**). (**J** through **M**) Rabbit retina shows a similar response as that seen in the cat. Induction of FRAs is apparent in both the INL and in some photoreceptor cells (*arrowheads*; **K**). Double labeling (**L**, **M**) for FRA (*arrowheads*) and vimentin (*arrows*) demonstrates FRA induction in Müller cells after RD. Scale bar, (**A** through **G**, **J** through **M**) 30 μm; (**H** and **I**) 20 μm.

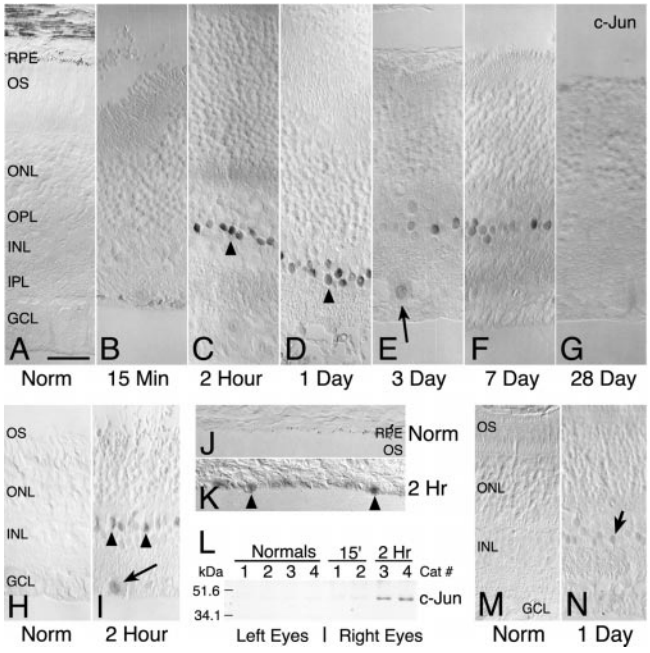

FIGURE 6. c-Jun immunolabeling increases in both RPE and INL cells after RD. The time course is virtually identical with that for c-Fos (Fig. 5). Normal (**A**) and 15 minutes detached (**B**) cat retina show essentially no immunoreactivity. c-Jun immunolabeling dramatically increases in INL cells at 2 hours and 1 day after RD (*arrowheads*; **C**, **D**). This labeling peaks around 1 day (**D**), remains highly induced at 3 (*arrow*, **E**) and 7 days (**F**), and declines to near normal levels by 28 days of RD (**G**). c-Jun immunolabeling of 2 hours detached rabbit retina (**H** and **I**) shows c-Jun induction in the INL (*arrowheads*; **I**) and the occasional ganglion cell (*arrow*; **I**). (**J** and **K**) c-Jun induction in cat RPE cells within 2 hours (*arrowheads*; **K**). Immunoblotting (**L**) confirms that c-Jun is induced by 2 hours of RD. An antibody to phospho-c-Jun (**M**, **N**) lightly labels INL cells (*arrow*; **N**) in a pattern that parallels increased c-Jun immunoreactivity (**I**). Scale bar, (**A** through **I**, **M**, and **N**) 30 μm; (**J** and **K**) 25 μm.

DISCUSSION

Data presented here suggest that Müller and RPE cells respond immediately to experimental RD. These nonneuronal retinal cells signal in response to RD via the ERK (p42/p44 MAP kinase) pathway and rapidly induce expression of AP-1, a critical transcription factor for numerous cellular processes. Our data implicate FGF-2 and FGFR1 as candidate molecules for initiating reactive cellular changes, which often lead to both gross and microscopic structural reorganization throughout the retina.

FGF-2 is expressed in the retina[24–26] and has been shown to stimulate gliosis and protein expression changes[27] after RD.[9] FGFR1 is present in both Müller and RPE cells,[28,29] and exogenous in vivo addition of FGF-2 leads to FGF receptor internalization, Müller cell proliferation, and increased expression of two intermediate filaments, glial fibrillary acidic protein and

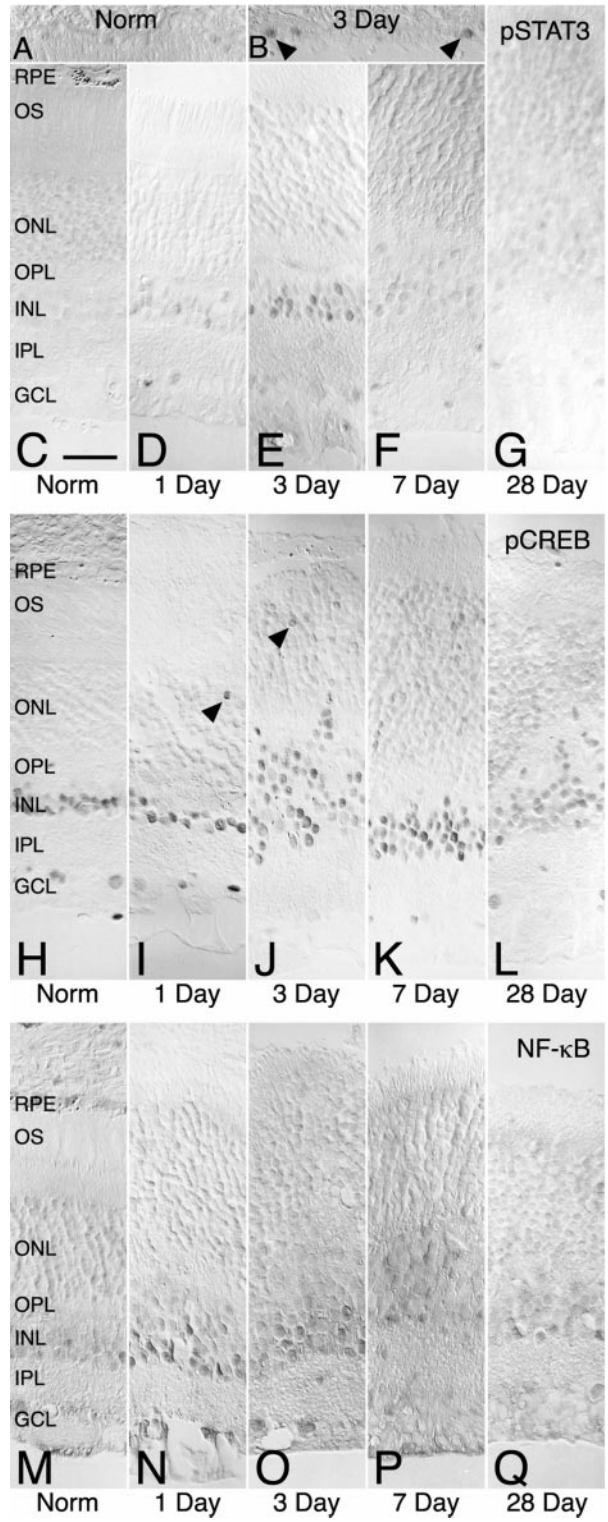

FIGURE 7. Immunohistochemical analysis of secondary signaling changes in response to RD in the cat; STAT3 and CREB are phosphorylated (pSTAT3 and pCREB, respectively), and NF-κB is activated after RD. (**A** through **G**) pSTAT3 immunohistochemistry. (**A**) No labeling in normal RPE, whereas (**B**) shows some pSTAT3 labeled RPE cells 3 days after RD (*arrowheads*; **B**). Normal retina (**C**) shows virtually no pSTAT3 immunoreactivity. Within 1 day (**D**), modest pSTAT3 immunoreactivity is detected some INL and GCL cells. INL cells are clearly immunopositive by 3 days (**E**); however, pSTAT3 labeling decreases at 7 day (**F**) and returns to near normal levels by 28 days after RD (**G**). (**H** through **L**) pCREB immunohistochemistry. Normal retina (**H**) shows pCREB immunoreactivity in both INL and GCL cells. At 1 (*arrowhead*; **I**), 3 (*arrowhead*; **J**), and 7 days (**K**) after RD, some photoreceptors are pCREB immunopositive. pCREB immunoreactivity returns to near normal levels by 28 days after RD (**L**). (**M** through **Q**) Activated NF-κB immunohistochemistry. Light immunoreactivity is seen throughout the normal retina (**M**), and by 1 day after RD (**N**) some INL cells show increased immunoreactivity. This trend continues at 3 (**O**) and 7 days (**P**), and returns to normal levels of activation by 28 days after RD (**Q**). Scale bar, (**A** through **Q**) 30 μm.

vimentin.[9] We show that FGFR1 becomes phosphorylated within 15 minutes and largely dephosphorylated 2 hours after RD (Fig. 1), suggesting that endogenous FGF-2 acts immediately in response to injury.

MAPK pathways are highly conserved intracellular signal transduction pathways that communicate information between the plasma membrane and nucleus.[30,31] Here we show that ERK is present in the retina, and it changes its cellular localization from the cytoplasm to the nucleus after RD (Fig. 2). ERK is rapidly phosphorylated (Fig. 3) in both Müller and RPE cells and persists in Müller cells for >7 days, indicating that these cells remain reactive for some time after injury. Indeed some components of the Müller cell gliotic response (hypertrophy, migration, and increased expression of intermediate filaments) remain dynamic for as long as the retina is detached,[23] while responses such as proliferation decrease to near background levels after 7 days.[4,6]

Concomitant with ERK phosphorylation, *c-fos* mRNA expression increases in both retina and RPE (Fig. 4). Shortly thereafter, both protein subunits of the AP-1 complex (c-Fos and c-Jun) become highly expressed in Müller cells (Figs. 5, 6). This increase in *c-fos* mRNA in the INL has also been shown in a model of penetrating focal injury.[17] Members of the Fos and Jun families frequently become activated and up-regulated in response to mitogenic stimuli and often serve as early-responding global regulators of gene expression.[32] Although we have not shown a direct link between AP-1 expression and the cellular changes induced by RD, it is known that AP-1 induction is necessary for proliferation to occur in other cell types,[32] and we have identified AP-1 induction in both Müller and RPE cells before they enter the cell cycle.[4,6] Other studies have suggested similar relationships among these molecules: FGFR1 signaling, ERK activation, and *c-fos* induction[33,34] have all been linked with a proliferative response.[35]

Additional signaling pathways also become activated in response to RD. Activation-specific antibodies to STAT3, CREB, and NF-κB, each demonstrate increased immunoreactivity within 3 days after RD, in a time frame consistent with their potential for contributing to secondary cellular changes. All three of these proteins have the capacity to respond to multiple stimuli, including growth factors and cytokines, and all are implicated in regulating a vast array of cellular responses.[36–40] The phosphorylation of STAT3 occurs in INL cells at 1 and 3 days after RD, a time that correlates temporally with Müller cell proliferation and intermediate filament expression.[4,5,41] CREB has been shown previously to become phosphorylated after penetrating retinal injury[42] and has been linked with c-Fos expression.[15] In this study, pCREB labeling is observed not only in INL cells, but also in some photoreceptors in a pattern reminiscent of apoptotic cell death after RD, that is, sparse and seemingly randomly scattered cells throughout the ONL.[7] Furthermore, we find increased NF-κB activation 1 to 3 days after RD in INL cells. NF-κB is known to become activated in response to a variety of stimuli including oxidative stress;[43,44]; a phenomenon that undoubtedly occurs rapidly in detached retina once it is separated from the choroidal circulation.[45,46]

The dedifferentiation and proliferation of the RPE, intra- and subretinal Müller cell proliferation (proliferative vitreoretinopathy, subretinal fibrosis), and loss of photoreceptors and their connectivity[47] may all contribute to abnormal information processing and blindness in the affected area.[8,47,48] In this study we aimed to identify components of signaling pathways that may be responsible for initiating the multi-facetted cellular responses to RD. Based on current evidence, we hypothesize that RD causes the rapid release of FGF-2 from intra- and/or extra-cellular stores, leading to the activation of FGFR1 and ERK, and proximate induction of c-Fos and c-Jun protein expression in both RPE and Müller cells. Based on numerous studies of AP-1, it is likely that increased AP-1 expression regulates a variety of secondary genetic and cellular responses. Furthermore, the activation of secondary signaling events suggests that a variety of stimuli contribute to the retina's longer-term responses to RD. Targeting such early signaling and transcriptional events with pharmaceutical intervention after RD in humans may help to reduce downstream cellular effects such as proliferation and apoptosis, before and/or after surgical correction.

Acknowledgments

The authors thank Brett Wilson for his excellent technical assistance and Don Anderson, Stu Feinstein, Beth Hinkle, Monte Radeke, and Frank Lovicu for their insight and comments and for providing reagents.

References

1. Burton TC. Preoperative factors influencing anatomic success rates following retinal detachment surgery. *Trans Am Acad Ophthalmol Otolaryngol.* 1977;83:499–505.
2. Tani P, Robertson DM, Langworthy A. Prognosis for central vision and anatomic reattachment in rhegmatogenous retinal detachment with macula detached. *Am J Ophthalmol.* 1981;92:611–620.
3. Hjelmeland L, Harvey A. Gliosis of the mammalian retina: migration and proliferation of retinal glia. In: Osborne N, Chader J, eds. *Progress in Retinal Research*. Vol. 7. Oxford: Pergamon Press; 1988:259–281.
4. Fisher SK, Erickson PA, Lewis GP, Anderson DH. Intraretinal proliferation induced by retinal detachment. *Invest Ophthalmol Vis Sci.* 1991;32:1739–1748.
5. Lewis GP, Guérin CJ, Anderson DH, Matsumoto B, Fisher SK. Rapid changes in the expression of glial cell proteins caused by experimental retinal detachment. *Am J Ophthalmol.* 1994;118:368–376.
6. Geller SF, Lewis GP, Anderson DH, Fisher SK. Use of the MIB-1 antibody for detecting proliferating cells in the retina. *Invest Ophthalmol Vis Sci.* 1995;36:737–744.
7. Cook B, Lewis GP, Fisher SK, Adler R. Apoptotic photoreceptor degeneration in experimental retinal detachment. *Invest Ophthalmol Vis Sci.* 1995;36:990–996.
8. Lewis GP, Linberg KA, Fisher SK. Neurite outgrowth from bipolar and horizontal cells after experimental retinal detachment. *Invest Ophthalmol Vis Sci.* 1998;39:424–434.
9. Lewis GP, Erickson PA, Guérin CJ, Anderson DH, Fisher SK. Basic fibroblast growth factor: a potential regulator of proliferation and intermediate filament expression in the retina. *J Neurosci.* 1992; 12:3968–3978.
10. Faktorovich EG, Steinberg RH, Yasumura D, Matthes MT, LaVail MM. Basic fibroblast growth factor and local injury protect photoreceptors from light damage in the rat. *J Neurosci.* 1992;12:3554–3567.
11. LaVail MM, Unoki K, Yasumura D, Matthes MT, Yancopoulos GD, Steinberg RH. Multiple growth factors, cytokines, and neurotrophins rescue photoreceptors from the damaging effects of constant light. *Proc Natl Acad Sci USA.* 1992;89:11249–11253.
12. Lewis GP, Linberg KA, Geller SF, Guérin CJ, Fisher SK. Effects of the neurotrophin brain-derived neurotrophic factor in an experimental model of retinal detachment. *Invest Ophthalmol Vis Sci.* 1999;40:1530–1544.
13. Wahlin KJ, Campochiaro PA, Zack DJ, Adler R. Neurotrophic factors cause activation of intracellular signaling pathways in Müller cells and other cells of the inner retina, but not photoreceptors. *Invest Ophthalmol Vis Sci.* 2000;41:927–936.
14. Curran T. The fos oncogene. In: Reddy EP, Skalka AM, Curran T, eds. *The Oncogene Handbook*. Amsterdam: Elsevier; 1988:307–325.
15. Sheng M, McFadden G, Greenberg ME. Membrane depolarization and calcium induce *c-fos* transcription via phosphorylation of transcription factor CREB. *Neuron.* 1990;4:571–582.
16. Sagar SM, Edwards RH, Sharp FR. Epidermal growth factor and transforming growth factor alpha induce c-Fos gene expression in retinal Müller cells in vivo. *J Neurosci Res.* 1991;29:549–559.

17. Yoshida K, Muraki Y, Ohki K, et al. *c-fos* gene expression in rat retinal cells after focal retinal injury. *Invest Ophthalmol Vis Sci.* 1995;36:251–254.
18. de Juan E Jr, Loewenstein A, Bressler NM, Alexander J. Translocation of the retina for management of subfoveal choroidal neovascularization ii: a preliminary report in humans. *Am J Ophthalmol.* 1998;125:635–646.
19. Lewis H, Kaiser PK, Lewis S, Estafanous M. Macular translocation for subfoveal choroidal neovascularization in age-related macular degeneration: a prospective study. *Am J Ophthalmol.* 1999;128: 135–146.
20. Anderson DH, Guérin CJ, Erickson PA, Stern WH, Fisher SK. Morphological recovery in the reattached retina. *Invest Ophthalmol Vis Sci.* 1986;27:168–183.
21. Cattoretti G, Pileri S, Parravicini C, et al. Antigen unmasking on formalin-fixed, paraffin-embedded tissue sections. *J Pathol.* 1993; 171:83–98.
22. Biroc SL, Murphy-Erdosh C, Fisher JM, Payan DG. The use of 33p-labeled oligonucleotides for in situ hybridization of vertebrate embryo frozen sections. *BioTechniques.* 1993;15:250–254.
23. Lewis GP, Erickson PA, Guérin CJ, Anderson DH, Fisher SK. Changes in the expression of specific Müller cell proteins during long-term retinal detachment. *Exp Eye Res.* 1989;49:93–111.
24. Wen R, Song Y, Cheng T, et al. Injury-induced upregulation of bFGF and CNTF mRNAs in the rat retina. *J Neurosci.* 1995;15: 7377–7385.
25. Cao W, Wen R, Li F, Lavail MM, Steinberg RH. Mechanical injury increases bFGF and CNTF mRNA expression in the mouse retina. *Exp Eye Res.* 1997;65:241–248.
26. Wen R, Cheng T, Song Y, et al. Continuous exposure to bright light upregulates bFGF and CNTF expression in the rat retina. *Curr Eye Res.* 1998;17:494–500.
27. Cao W, Wen R, Li F, Cheng T, Steinberg RH. Induction of basic fibroblast growth factor mRNA by basic fibroblast growth factor in Müller cells. *Invest Ophthalmol Vis Sci.* 1997;38:1358–1366.
28. Yamamoto C, Ogata N, Matsushima M, et al. Gene expressions of basic fibroblast growth factor and its receptor in healing of rat retina after laser photocoagulation. *Jpn J Ophthalmol.* 1996;40: 480–490.
29. Guillonneau X, Regnier-Ricard F, Laplace O, et al. Fibroblast growth factor (FGF) soluble receptor 1 acts as a natural inhibitor of FGF2 neurotrophic activity during retinal degeneration. *Mol Biol Cell.* 1998;9:2785–2802.
30. Bernstein LR, Ferris DK, Colburn NH, Sobel ME. A family of mitogen-activated protein kinase-related proteins interacts in vivo with activator protein-1 transcription factor. *J Biol Chem.* 1994; 269:9401–9404.
31. Widmann C, Gibson S, Jarpe MB, Johnson GL. Mitogen-activated protein kinase: conservation of a three-kinase module from yeast to human. *Physiol Rev.* 1999;79:143–180.
32. Angel P, Karin M. The role of Jun, Fos and the AP-1 complex in cell-proliferation and transformation. *Biochim Biophys Acta.* 1991; 1072:129–157.
33. Condorelli DF, Kaczmarek L, Nicoletti F, et al. Induction of protooncogene Fos by extracellular signals in primary glial cell cultures. *J Neurosci Res.* 1989;23:234–239.
34. Treisman R. Ternary complex factors: growth factor regulated transcriptional activators. *Curr Opin Genet Dev.* 1994;4:96–101.
35. Wang JK, Gao G, Goldfarb M. Fibroblast growth factor receptors have different signaling and mitogenic potentials. *Mol Cell Biol.* 1994;14:181–188.
36. Jaynes CD, Sheedlo HJ, Agarwal N, et al. Müller and retinal pigment epithelial (RPE) cell expression of NGFI-a and c-Fos mRNA in response to medium conditioned by the RPE. *Brain Res Mol Brain Res.* 1995;32:329–337.
37. Hill CS, Treisman R. Transcriptional regulation by extracellular signals: mechanisms and specificity. *Cell.* 1995;80:199–211.
38. Leaman DW, Pisharody S, Flickinger TW, et al. Roles of JAKs in activation of STATs and stimulation of c-fos gene expression by epidermal growth factor. *Mol Cell Biol.* 1996;16:369–375.
39. Andrisani OM. CREB-mediated transcriptional control. *Crit Rev Eukaryot Gene Expr.* 1999;9:19–32.
40. Mercurio F, Manning AM. Multiple signals converging on NF-kB. *Curr Opin Cell Biol.* 1999;11:226–232.
41. Kahn MA, Huang CJ, Caruso A, et al. Ciliary neurotrophic factor activates JAK/STAT signal transduction cascade and induces transcriptional expression of glial fibrillary acidic protein in glial cells. *J Neurochem.* 1997;68:1413–1423.
42. Harada T, Imaki J, Hagiwara M, et al. Phosphorylation of CREB in rat retinal cells after focal retinal injury. 1995;61:769–772.
43. Maulik N, Sato M, Price BD, Das DK. An essential role of NF-κB in tyrosine kinase signaling of p38 MAP kinase regulation of myocardial adaptation to ischemia. *FEBS Lett.* 1998;429:365–369.
44. Yoshida A, Yoshida S, Hata Y, Khalil AK, Ishibashi T, Inomata H. The role of NF-kB in retinal neovascularization in the rat. Possible involvement of cytokine-induced neutrophil chemoattractant (CINC), a member of the interleukin-8 family. *J Histochem Cytochem.* 1998;46:429–436.
45. Mervin K, Valter K, Maslim J, Lewis G, Fisher S, Stone J. Limiting photoreceptor death and deconstruction during experimental retinal detachment: the value of oxygen supplementation. *Am J Ophthalmol.* 1999;128:155–164.
46. Linsenmeier RA, Padnick-Silver L. Metabolic dependence of photoreceptors on the choroid in the normal and detached retina. *Invest Ophthalmol Vis Sci.* 2000;41:3117–3123.
47. Fisher SK, Anderson DH. Cellular effects of detachment on the neural retina and retinal pigment epithelium. In: Ryan SJ, ed. *Retina*. Third Edition, Vol. 3. St. Louis: Mosby; 2001:1961–1986.
48. Fisher SK, Anderson DH. Cellular responses of the retinal pigment epithelium to retinal detachment and reattachment. In: Marmour MF, Wolfensberger TJ, eds. *The Retinal Pigment Epithelium*. New York: Oxford University Press; 1998:406–419.